Adsorption and dissociation of hydrogen molecules on a Pt atom on defective carbon nanotubes

Yongjin Park, Gunn Kim, and Young Hee Lee[a)]
BK21 Physics Division, Department of Physics, Center for Nanotubes and Nanostructured Composites, Sungkyunkwan Advanced Institute of Nanotechnology, Sungkyunkwan University, Suwon 440-746, Korea

(Received 20 November 2007; accepted 8 January 2008; published online 28 February 2008)

Using density functional calculations, we investigate the catalytic effect of a Pt atom on a defective carbon nanotube. The Pt atom binds more strongly to the vacancy site than to the Stone-Wales defect and to the pure surface of the nanotube. The binding energy of the H_2 molecule on the vacancy is significantly reduced to 0.68 eV from 1.26 eV of the pure (5,5) nanotube but still sufficient enough to maintain minimum bond strength on the Pt atom. Moreover, the H–H distance is separated to 2.16 Å. The feasibility to the fuel cell is further discussed. © *2008 American Institute of Physics*. [DOI: 10.1063/1.2838732]

A fuel cell is a promising device to harvesting energy from various materials such as methanol and hydrogen gases. Nevertheless, one serious drawback of the fuel cell is associated with the catalyst. Despite high catalytic efficiency, Pt nanoparticles are expensive and limited natural resources. To minimize the amount of Pt catalysts, the formation of efficient Pt nanoparticles less than 3 nm is prerequisite prior to the practical applications.[1] A uniform distribution of Pt nanoparticles on the supporting electrodes and their high conductivity are also of crucial importance to prevent Pt nanoparticles from being aggregated themselves.[2] Another important criterion of the supporting electrodes is the high conductivity so that the electrons that are harvested should be efficiently collected by the electrodes to be used for energy source.[3,4]

For this reason, a carbon nanotube (CNT) has been a strong candidate as a supporting electrode. Recently, Pt nanoparticles less than 3 nm have been successfully loaded on defective CNTs using microwave treatment.[5] An alternative approach of using different catalysts such as TiH_2 on polymers has been also suggested. The catalyst for the fuel cell should (i) dissociate efficiently the incoming molecular hydrogen (H_2) gas during adsorption and (ii) have the reasonable binding energy with incoming materials so that they can be easily desorbed at moderate temperature.

Our main goal here is to search for a possibility of reducing Pt nanoparticle size further and possibly at the atomic scale. In this letter, by introducing some defective sites such as the Stone-Wales (SW) defect[6] and the monovacancy (the single vacancy) on the CNT wall and adsorbing the Pt atom on such defects, we perform density functional calculations[7,8] to know which site is more effective for catalysis. Our calculations demonstrate that the H_2 molecule on the Pt atom at the vacancy site of the CNT can be almost dissociated into an atomic state with a separation of greater than 2 Å and furthermore their binding energy is significantly reduced compared to those of the SW defect and the pure CNT.

The first-principles pseudopotential calculations were performed based on the density functional theory within the generalized gradient approximation[9,10] implemented in the DMOL3 package.[11] We used the double numerical quality basis set with a polarization *d* function. Norm-conserving DFT semicore pseudopotentials are employed to the core and valance electrons.[12,13] We treated four times primitive cell for (5,5) CNTs and two times primitive cell for (8,0) CNTs in the tube axis direction to reduce the adsorbate-adsorbate interaction. The supercells have the lattice constant of 20 Å in the lateral direction to neglect the interaction between adjacent nanotubes. The Brillouin zone is sampled with a $1\times1\times6$ irreducible Monkhorst-Pack *k*-point grid.[14] The binding energy of Pt $[E_b(\mathrm{Pt})]$ was calculated as the difference of total energies between an adsorbed system and the separate species, $E_b(\mathrm{Pt})=E(\mathrm{Pt+CNT})-E(\mathrm{CNT})-E(\mathrm{Pt})$, and for H_2 binding energy on Pt-CNT, E_b (H_2) as $E_b(H_2)=E(H_2+\mathrm{Pt}+\mathrm{CNT})-E(\mathrm{Pt+CNT})-E(H_2)$, where $E(\alpha)$ is the total energy of a given system. We also carried out the reference calculations using the OPENMX code,[15] and the overall results are in agreement with the data from the DMOL3 code.

Figure 1 shows the fully relaxed geometries of the H_2-adsorbed Pt atoms which are located on various defects

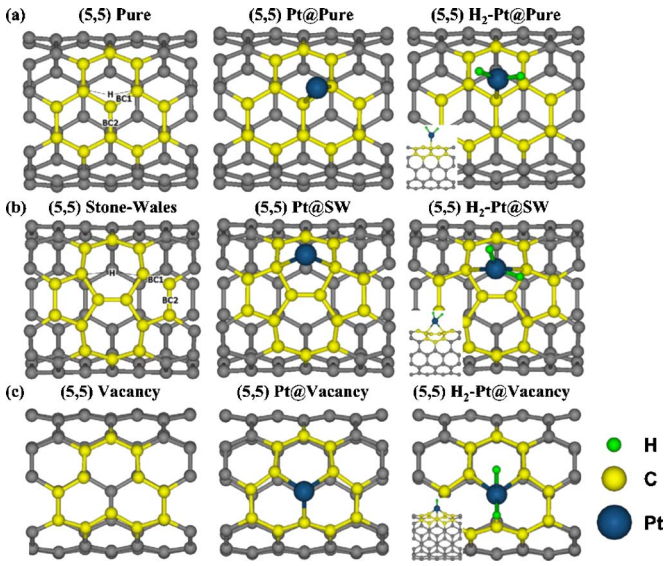

FIG. 1. (Color online) The optimized geometries of the Pt atom and the H_2 molecule adsorbed on (a) the (5,5) pure CNT, (b) the (5,5) Stone-Wales CNT, and (c) the (5,5) vacancy CNT. The leftmost panels indicate possible adsorption sites of the Pt atom.

[a)]Author to whom correspondence should be addressed. Electronic mail: leeyoung@skku.edu.

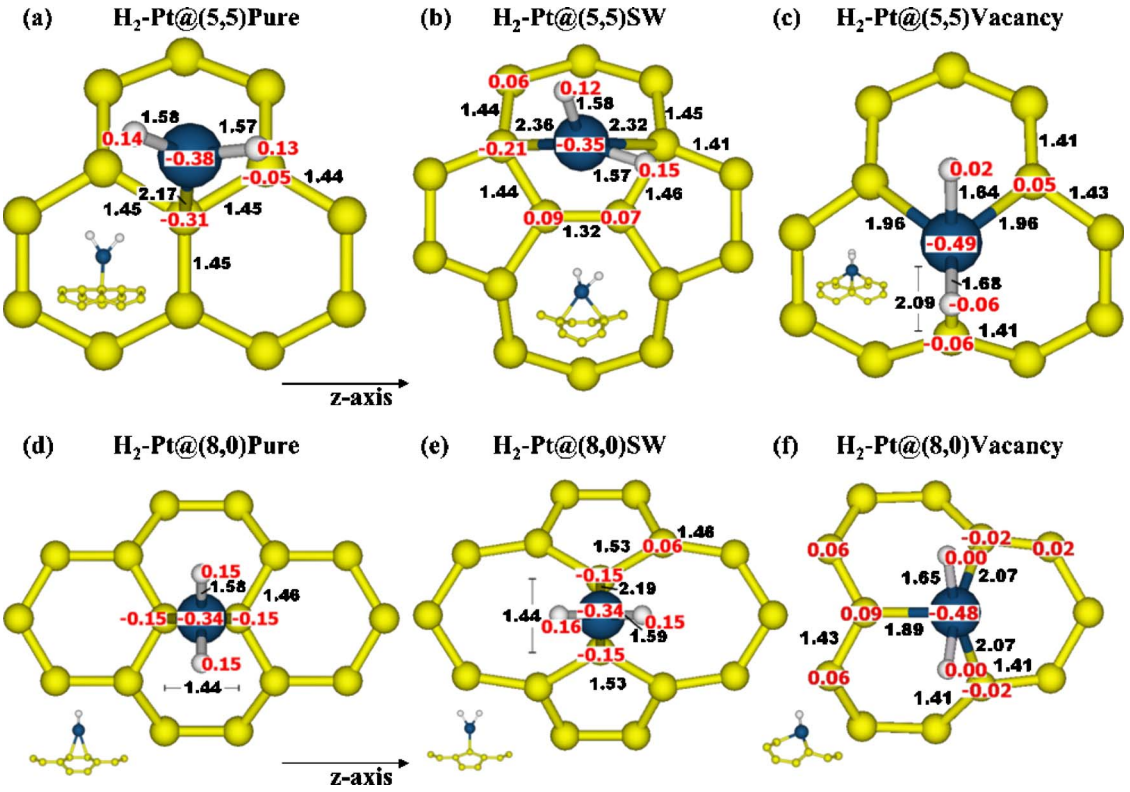

FIG. 2. (Color online) The detailed local geometries and the amount of charge transfers near the Pt atom for (a) H_2–Pt-(5,5) pure CNT, (b) H_2–Pt-(5,5) SW CNT, and (c) H_2–Pt-(5,5) vacancy. (d)–(f) are similar for the (8,0) CNT. The insets indicate the side views of the geometries. The numbers (red in online color) on the atoms represent the amount of charge transfer by Mulliken charge population in unit of $|e|$. Bond lengths are also shown in the figures and in unit of angstroms.

of (5,5) CNTs. Three stable adsorption sites for the Pt atom were found in the pure (5,5) CNT. The binding energies of these bond-centered (BC1 and BC2) and hexagonal (H) sites are 2.53, 2.35, and 2.45 eV, respectively [Fig. 1(a)]. For H site, the Pt atom is closely located to the adjacent carbon atom. The most stable site is BC1 with Pt–C bond length of 2.08 Å, which is similar to previous results.[16] The hydrogen molecule is then added to the most stable BC1 configuration with a vertical separation distance of ~1.6 Å from the Pt atom. While the hydrogen molecule is adsorbed with an activation barrier height from the transition state calculations, it binds to the Pt atom with a binding energy of 1.26 eV and Pt–H bond length of 1.57 Å and other local geometries listed in Fig. 2(a). In this case, the hydrogen bond length is expanded to 1.88 Å from the molecular bond length of 0.75 Å. However, for (8,0) pure CNT, the position of Pt atom on the bridge site was not changed during hydrogen adsorption shown in Fig. 2(d). In this structure, the configuration of the hydrogen molecule is symmetric, compared with (5,5) pure CNT.

The SW (5-7-7-5) defect is illustrated in Fig. 1(b). Three stable adsorption sites for Pt atoms, two bond centers and one (shifted) heptagon site, are found in this case. The heptagon site is the most stable geometry with a binding energy of 2.86 eV, which is stronger than that of the pure nanotube by ~0.4 eV. Two carbon atoms having a bridging form with the Pt atom are pushed downward (side view), as shown in Fig. 2(b) even before hydrogen adsorption. The adsorption of the H_2 molecule was exothermic with no practical activation barrier similar to that of the pure CNT. The binding energy of the hydrogen molecule is 0.95 eV with a Pt–H bond length of 1.57 Å. The local geometries of the SW defect and hydrogen-adsorbed defect are similar to those of the pure CNT except the adsorption site. On the other hand, for (8,0) SW, the center bridge site is the most stable for Pt atom and the configuration of hydrogen molecule is symmetric compared with the case of (5,5) SW shown in Fig. 2(e).

For a monovacancy, in Fig. 1(c), the positions of atoms near the vacancy were not much deviated from those of the pure CNT. A single adsorption site of the Pt atom is available only at the monovacancy site. The energy gain is huge with a binding energy of 6.56 eV, by removing dangling bonds from vacancy. Adsorption of the hydrogen molecule is again exothermic with no practical activation barrier. The hydrogen binding energy is significantly reduced to 0.68 eV compared to 1.26 eV of the pure nanotube. The Pt–H bond length increased by ~0.1 Å due to the reduction of charge transfer at hydrogen atoms. Hydrogen charges are less depleted compared to that of Stone-Wales. The H–H distance is further separated to 2.16 Å. For the monovacancy defects of both (5,5) and (8,0) CNTs, hydrogen molecules are adsorbed perpendicular to the longitudinal axis of the CNT, as shown in Figs. 2(c) and 2(f). The trend of the changes in the binding energy of H_2–Pt and H–H separation distance in a semiconducting (8,0) CNT is similar to that of the metallic (5,5) CNT, as displayed in Fig. 2(b) and Table I.

To understand the energetics and the related electronic structures of hydrogen adsorption on Pt-adsorbed CNT surface, the density of states (DOS) was calculated for H_2–Pt-pure and H_2–Pt-vacancy (Fig. 3) using the OPENMX code. The local density of states (LDOS) of H_2 and Pt clearly shows the difference in the electronic structures of two structures. For H_2–Pt-pure, p and d levels of the Pt atom are located around −0.5 eV (below the Fermi level), whereas the

TABLE I. The binding energies of the Pt atom on the (5,5) pure, the defective CNTs, and the H_2 molecule on the Pt-(5,5) pure CNT, and the Pt-(5,5) defective CNT. The bond lengths between H atoms and the angles of H–Pt–H.

	H_2 adsorption site	$E_b^{\text{Pt–CNT}}$ (eV) GGA	$E_b^{\text{Pt–H2–CNT}}$ (eV) GGA (LDA)	$L_{\text{H–H}}$ (Å) GGA (LDA)	$\angle_{\text{H–Pt–H}}$ (deg)
(5,5)	Pt-pure	2.53	1.26(1.87)	1.88(1.89)	73.5
	Pt-Stone-Wales	2.86	0.95(1.64)	1.91(1.90)	74.6
	Pt-vacancy	6.56	0.68(1.16)	2.16(2.16)	81.3
(8,0)	Pt-pure	2.75	1.04(1.56)	1.74(1.74)	66.7
	Pt-Stone-Wales	3.28	0.85(1.42)	1.61(1.67)	63.7
	Pt-vacancy	6.40	0.78(1.22)	2.20(2.20)	83.5

s levels of H_2 are located deep in the valence band, revealing no coupling between the H_2 molecule and the Pt atom. On the other hand, for H_2–Pt-vacancy, *s* levels in the H_2 molecule are located with *p* and *d* levels in the Pt atom below −1.5 eV. It means that they are strongly hybridized with each other. The large H–H separation distance and weak binding energy of H_2 on Pt-vacancy compared to those of H_2 on Pt-pure can be explained in conjunction with the charge populations.

The Mulliken charge populations of the Pt atom and two H atoms in Pt-pure and H_2–Pt-vacancy are analyzed. The electrons are transferred from CNTs to the Pt atom because of the difference of the electron affinity. The weaker binding energy of H_2 on Pt-vacancy can be explained in terms of stronger Pt–C binding and a negligible charge transfer between Pt atoms and H_2. Compared to Pt-pure, the Pt atom in Pt-vacancy obtains more electrons from the CNT (by $\sim 0.1e$). The significant dipole interaction is associated with the Pt–C binding. For the negligible charge transfer between Pt atoms and H_2 molecule, this is in good contrast with the case of H_2 on Pt-pure, where a considerable amount of charge transfer ($0.2–0.3e$) from H_2 to the Pt atom is noticed, and therefore large portion of dipole energy strengthens the H_2 binding energy on Pt-pure. On the other hand, the H–H separation distance is correlated to the coupling between Pt and H atoms. The occupation number of *p* orbitals is increased, whereas that of *d* orbitals is decreased in Pt-vacancy. As a consequence, the occupation increase of *p* orbitals and the occupation decrease of *d* orbitals modify the bond angle (<H–Pt–H).

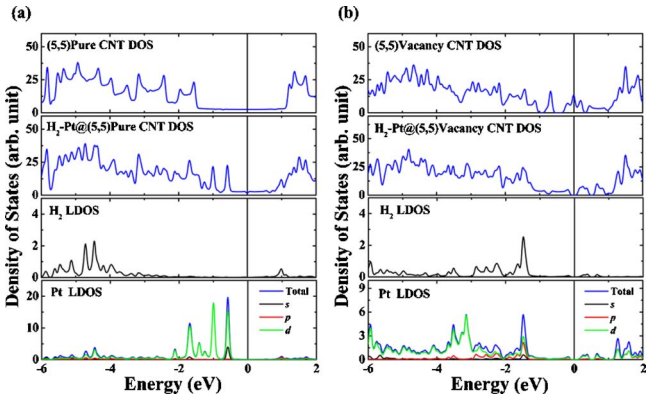

FIG. 3. (Color online) The DOS of (a) the (5,5) pure and the H_2–Pt-(5,5) pure CNT and (b) the (5,5) vacancy and the H_2–Pt-(5,5) vacancy CNT. The LDOS of states of H_2 and Pt for *s*, *p*, and *d* orbitals are also shown in the bottom panels.

In summary, we have investigated adsorption nature of the hydrogen molecule on the Pt atom at the defect such as the Stone-Wales defect and the monovacancy. Our results reveal that the hydrogen molecule binds less strongly and the H–H bond became weaker on Pt-vacancy than those on Pt-pure. These differences in the binding energy and the H–H separation distance originate from the charge transfer and the strong coupling between H_2 and the Pt atom. This opens a new possibility of using the Pt atom on a vacancy of CNTs as a new type of catalyst, which is advantageous over the large sized Pt aggregates.

This work was supported by the Ministry of Education through the STAR-faculty project and the KOSEF through the CNNC at SKKU.

[1] G. G. Wildgoose, C. E. Banks, and R. G. Compton, Small **2**, 182 (2006).
[2] V. Georgakilas, D. Gournis, V. Tzitzios, L. Pasquato, D. M. Guldi, and M. Prato, J. Mater. Chem. **17**, 2679 (2007).
[3] S. J. Tans, R. M. Verschueren, and C. Dekker, Nature (London) **393**, 49 (1998).
[4] K. H. An and Y. H. Lee, NANO **1**, 115 (2006).
[5] S. J. Kim, Y. J. Park, E. J. Ra, K. K. Kim, K. H. An, Y. H. Lee, J. Y. Choi, C. H. Park, S. K. Doo, M. H. Park, and C. W. Yang, Appl. Phys. Lett. **90**, 023114 (2007).
[6] A. J. Stone and D. J. Wales, Chem. Phys. Lett. **128**, 501 (1986).
[7] P. Hohenberg and W. Kohn, Phys. Rev. **136**, B864 (1964).
[8] W. Kohn and L. J. Sham, Phys. Rev. **140**, A1133 (1965).
[9] J. P. Perdew and W. Yue, Phys. Rev. B **33**, 8800 (1986).
[10] J. P. Perdew and W. Yue, Phys. Rev. B **45**, 13244 (1992).
[11] MATERIALS STUDIO (version 4.1) of Accelrys Inc.
[12] D. M. Ceperley and B. J. Alder, Phys. Rev. Lett. **45**, 566 (1980); J. P. Perdew and A. Zunger, Phys. Rev. B **23**, 5048 (1981).
[13] L. Kleinman and D. M. Bylander, Phys. Rev. Lett. **48**, 1425 (1982).
[14] H. J. Monkhorst and J. D. Pack, Phys. Rev. B **13**, 5188 (1976).
[15] DFT OPENMX code is available on the web site http://www.openmx-square.org/
[16] G. Chen and Y. Kawazoe, Phys. Rev. B **73**, 125410 (2006).